SCIENTIFIC REPORTS

OPEN

SUBJECT AREAS:
SUPER-RESOLUTION MICROSCOPY
DIAGNOSTIC DEVICES

Received
28 January 2014

Accepted
24 July 2014

Published
12 August 2014

Correspondence and requests for materials should be addressed to E.K. (waterlake@mail.ru)

Transformation of membrane nanosurface of red blood cells under hemin action

Elena Kozlova, Alexander Chernysh, Victor Moroz, Olga Gudkova, Victoria Sergunova & Artem Kuzovlev

V.A. Negovsky Scientific Research Institute of General Reanimatology RAS, Moscow, Russian Federation.

Hemin is the product of hemoglobin oxidation. Some diseases may lead to a formation of hemin. The accumulation of hemin causes destruction of red blood cells (RBC) membranes. In this study the process of development of topological defects of RBC membranes within the size range from nanoscale to microscale levels is shown. The formation of the grain-like structures in the membrane ("grains") with typical sizes of 120–200 nm was experimentally shown. The process of formation of "grains" was dependent on the hemin concentration and incubation time. The possible mechanism of membrane nanostructure alterations is proposed. The kinetic equations of formation and transformation of small and medium topological defects were analyzed. This research can be used to study the cell intoxication and analyze the action of various agents on RBC membranes.

Oxygen delivery to the tissues is the key function of red blood cells (RBC). Under the physiological conditions the majority of RBC are represented by discocytes. Endogenous and exogenous factors can affect their shape and transform them into stomatocytes, echinocytes, spherocytes etc[1]. The changes of cell shape affect its deformability which in turn influences on rheological properties of the blood. There is a certain sequence of steps in the transformation from discocytes to spheroechinocytes. Some studies indicate the structures of RBCs which are mostly affected by various physical or pharmacological agents. These cell structures are spectrin, membrane proteins or lipids[2–6]. But the mechanism of formation of membrane topologic defects which finally leads to the changes of cell shape and deformability is currently unclear.

The hemin is a substance which alters the morphology of cells. The objects of its action in RBC are known. The optical microscopy and electron microscopy showed that hemin causes a formation of echinocytes under low concentrations and spheroechinocytes under high concentrations[7]. Finally this leads to hemolysis. The hemin affects the conformation of spectrin, protein band 4.1 and weakens junctions between them[3–5]. This was proved by the electrophoresis and electron spin resonance methods[5]. A variety of disorders may lead to a formation of hemin, which in turn causes hemolysis[8–9].

The investigation of hemin action on the RBC membranes is of great significance for clinical nanomedicine. The hemin is a product of hemoglobin oxidation. Under blood loss heme oxidation occurs and hemoglobin is released from the RBC into the bloodstream. Malaria, sickle cell disease and ischemia lead to oxidation processes that result in formation of hemin and alterations of membranes. The hemin also arises under the action of stomach enzymes and hydrochloric acid on hemoglobin. Bleeding stomach erosions and ulcers are black due to the hemin presence[10]. A slow accumulation of hemin, a phenomenon increased in pathologically altered cells, is a toxic event causing RBC destruction[11]. Ionizing radiation also leads to oxidation and membrane desctruction[12], the formation of methemoglobin increases the probability of hemin appearance in the body.

The appearance of specific topological structures in RBC membrane under the hemin action was first demonstrated in our recent work[13]. The sizes of these structures were within the range of nanoscale level (nanoscale level means that the size of object is less than 100 nm in at least one dimension).

Characterization and dynamics of reorganization of topological structures within the membrane from nanoscale level (0.1–100 nm) to microscale levels (1–10 μm) up to the formation of spheroechinocytes was not yet investigated. In the current research we used an atomic force microscopy (AFM) which is most suitable for the membrane nanostructure evaluation[13].

The aim of the study was to describe the formation and determine the dynamics of topological defects of RBC membranes at the nanoscale and microscale levels as well as develop a model of membrane transformation under the hemin action.

Results

Transformation of cell morphology under the hemin action. The result of hemin action on cell may be unequal in different cells due to the heterogeneity of RBC and viscous microenvironment in blood. It is impractical to evaluate all the alterations arising in the membrane of each cell. Therefore to study the trends in membrane structure and cell shape alterations it is necessary to use the statistical methods to analyze time-dependent changes in an ensemble of cells under various hemin concentrations (C). We consider a number of cells in the monolayer of smear as a statistical ensemble. Thus the smear of cell monolayer seems to be an optimal object for this study.

In our experiments each monolayer contained at least 10^5 cells. Experiments were performed five times and three smears were made for each experimental series. Therefore typical shapes of cells and membrane surfaces for the given hemin concentration (C) and time of incubation (t) were reliably determined. The changes in the distribution of morhologically heterogenous cells under various hemin concentrations were studied. The representative (typical) cell shapes and membrane surface patterns were revealed by statistical processing.

A representative AFM image (100 × 100 μm) of cells in the control smear is shown in Fig. 1a. Forty five images, each including 60–100 cells, were analyzed for each hemin concentration and each incubation time. Scanning of the fields 30 × 30 μm (Fig. 1 a–f) and 10 × 10 μm (Fig. 2, 3) was performed for more detailed AFM images.

Fig. 1a–e represents the results for the first incubation time (60 min). In the control smear (without hemin, C=0) 95 ± 2% of cells were represented by discocytes (Fig. 1a). At C= 0.8 mM 85 ± 5% of cells in monolayer were represented by deformed discocytes and stomatocytes (Fig. 1b). Increasing the concentration up to C=1.2 mM resulted in 78 ± 6% of cells turned into planocytes (Fig. 1c). At the stage of planocytes, the unusual grain-like patterns ("grains") appeared in the membrane surface of some cells.

Further increase of the hemin concentration (C=1.5 mM) led to 84 ± 10% of planocytes, on whose surface the "grains" became evident. Topologically, the "grains" were organized on the cell membrane as separate domains. "Grains"-containing domains were surrounded by the usual topological structure similar to the control group membrane (Fig. 1d). The distance between the tops of neighboring "grains" within each domain varied within the range of 120–200 nm with the typical height of "grains" 7–17 nm. The appearance of "grains"-containing domains on RBC membrane under the hemin action was noticed for the first time in our previous study[13].

An increased hemin concentration led to the merging of the "grains"; similarly, domains merged (Fig. 1e). At C=2.5 mM in 79 ± 8% of cells "grains"-containing domains were merged. Some cells in this group with merged domains were represented by spheroechinocytes.

With the increase of hemin incubation time up to 3 hrs the percentage of cells is altered. At C=0.8 mM the planocytes (42 ± 7%) and stomatocytes (35 ± 5%) predominated in the monolayer of smear. Other detected cells were discocytes (12 ± 5%) or contained a deep cavity (11 ± 4%). At the C= 1.2 mM 60 ± 5% of the cells were represented by planocytes, and 25 ± 3% were cells with "grains"-containing domains. In 15 ± 4% of cells a phenomenon of merging of the domains associated with the echinocyte formation was detected. At C=1.5 mM 43 ± 6% of cells had domains, 46 ± 6% were echinocytes with merging domains and 11 ± 4% were classified as spheroechinocytes.

The dependence of "grains"-containing domains on the incubation time (t_1= 3 min, t_2= 60 min and t_3= 180 min) is shown in Fig. 1f at the same hemin concentration C=1.5 mM. If the incubation time was short (t_1= 3 min) the appearance of the first "grains" was observed. Increasing the hemin incubation time (t_2= 60 min) led to an appearance of clearly detectable "grains"-containing domains. Following a further incubation the merging of "grains" in domains and merging of domains themselves in most of the cells as well as the formation of spheroechinocytes was evident. It could be seen that a longer incubation times with 1.5 mM hemin caused an effect similar to the increase of hemin concentration. This phenomenon was mostly evident within the range of C= 1.2–1.7 mM. At C>2.2 mM the formation of echinocytes and spheroechinocytes occurred immediately after the addition of hemin. At C< 0.8 mM the "grains" did not appear at any time of incubation up to 180 min.

Therefore the increased concentration of hemin and time of incubation caused the transition from discocytes to spheroechinocytes (Fig. 1 a–f). The similar cell morphology as shown in Fig. 1a–c was detected after an exposure of blood to other physical and chemical agents, e.g. hypotonic and hypertonic solutions of NaCl, UV radiation, ionizing radiation, zinc ions, impulse electrical field, esmeron, surface active substances[1,13–15]. However, the hemin led to an appearance of nanostructured "grains" on the membrane surface. Alteration of cell shape after the hemin action, i.e. formation of echinocytes and spheroechinocytes, was detected by a light microscopy[7]. However, this approach does not allow to show the grain-like structures on the cell membrane.

Nanostructural topology of "grain" and "grains"-containing domains on the cell membrane. All the domains contained regular nanostructures as "grains". The formation of domains was always dependent on the hemin concentration at a threshold of 1.2–1.7 (±0.2 mM). Hemin at low concentrations did not induce domain structures while at increased concentrations "grains" became merged. Fig 2a demonstrates images of a typical control cell (no hemin), represented by a discocyte. The representative image of the nanostructure of its membrane is presented in Fig. 2b, and its profile is shown in Fig. 2c. Fig. 2d demonstrates the planocyte at an the onset of domain formation at the hemin concentration C=1.1–1.2 mM (60 min of incubation).The number of domains was low - 6 ± 3 per cell (Fig. 2d). The number of "grains" was 3 ± 2 per domain (Fig. 2e). Fig. 2f shows the profile of the "grain" nanostructure within the domain.

At an increased concentration of hemin up to 1.5 mM the number of domains on the membrane surface increased up to 15 ± 4 (Fig. 3a, AFM image 8 × 8 μm). The number of grains was 11 ± 6 per each domain (Fig. 3b,). The one-way ANOVA showed a statistically significant difference between the number of domains at C=1.2 mM and C= 1.5 mM and "grains" at these concentrations ($p<0.05$).

Fig 3b and Fig 3c demonstrate the nanostructure and profile of a typical domain in AFM image at enhanced resolution (scan field 1800 × 1800 nm). The latter profile demonstrates the periodical topology of "grains" within the domain. The typical size of the distance between neighboring "grains " L (space period) was 160 ± 40 nm. The height of each grain was 12 ± 5 nm. The sizes of domains varied from 300 nm to 1500 nm.

The formation of cells with "grains"-containing domains was highly reproducible. Fig. 4 demonstrates five cells each containing "grains" scanned by AFM. The examples of structures of separate domains and a separate "grain" structure are shown in Fig. 4b (AFM 2D-image) and in Fig. 4c (AFM 3D-image) respectively. The profiles of nanostructures of cell surface patterns in the control and hemin-treated membranes were different (Fig. 5a and Fig. 5b). The histogram of typical space periods L in the profile of the control membrane was bimodal (Fig. 5c) including two peaks L_{1max}= 80–90 nm and L_{2max}= 140–150 nm. After the hemin action the typical space period was unimodal with the peak 160–175 nm (Fig. 5d). The proposed mechanism of this phenomenon will be described in the Discussion section.

Transition of nanostructural patterns to microstructural topological defects within the cell membrane. The fusion of "grains" within the domains and domains with each other was detected

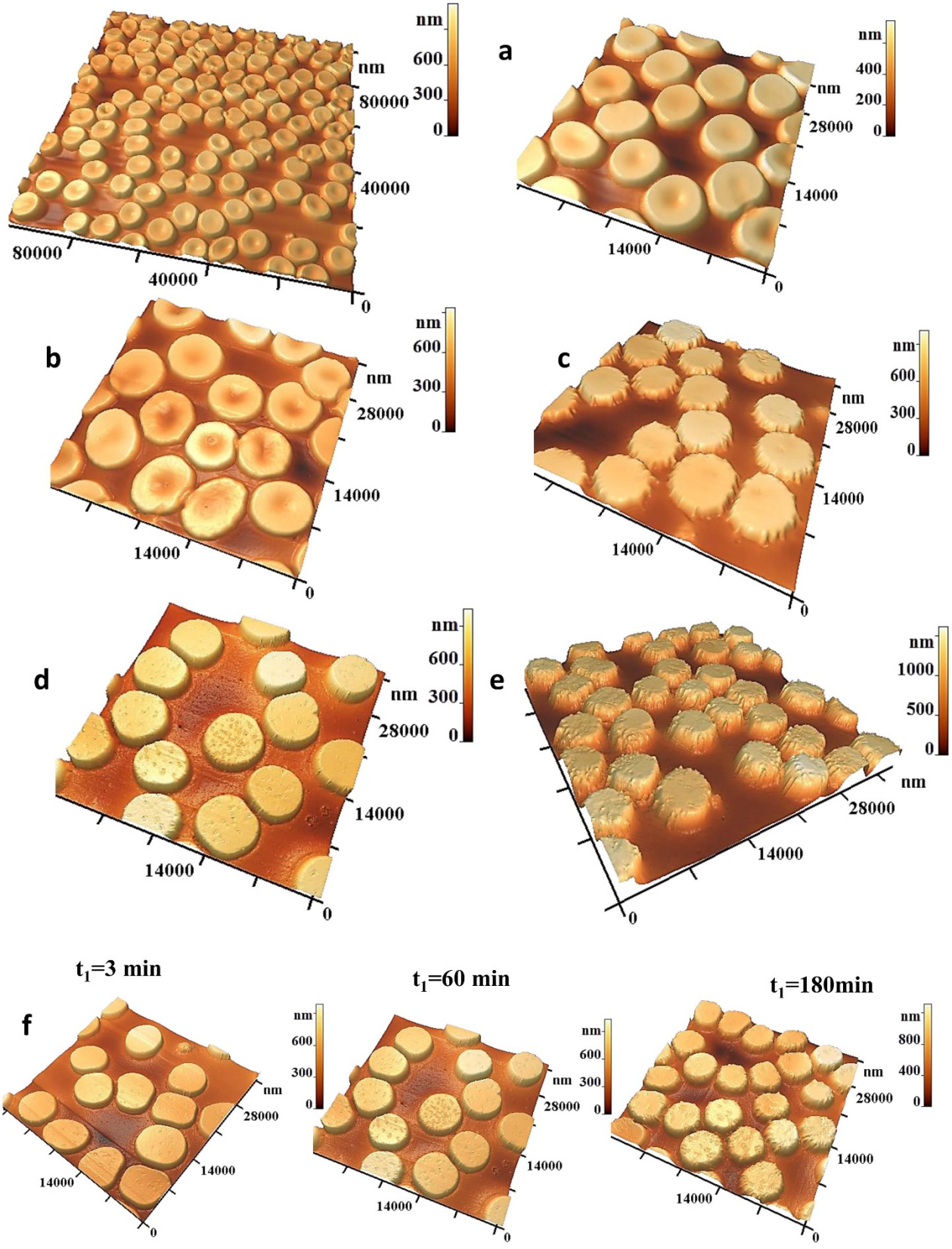

Figure 1 | Stages of transformation of RBC shape and its membrane under the hemin action for different concentrations C. (a) C = 0 (control), AFM 3D- images 100 × 100 μm and 30 × 30 μm of cells in control smear, 95 ± 2% discocytes. (b) C=0.8 mM, AFM 3D-images 30 × 30 μm, 85 ± 5% deformed discocytes and stomatocytes. (c) C=1.2 mM, AFM 3D-images 30 × 30 μm, 78 ± 6% planocytes and rising of topological "grain" defects. (d) C=1.5 mM, AFM 3D-images 30 × 30 μm, 84 ± 10% cells with "grains"-containing domains on the membrane surface. (e) C=2.5 mM, AFM 3D-images 30 × 30 μm, 79 ± 8% cells with merging domains and spheroechinocytes. Time of incubation was 60 min for (a–e). (f) The dependence of domains arising on incubation time t_i for the same hemin concentration C=1.5 mM (t_1= 3 min, t_2= 60 min and t_3= 180 min). Statistical processing performed by 100 × 100 μm AFM 3D-images of cells in monolayers in 45 smears. (60–100 cells in each image) for each concentration and each time.

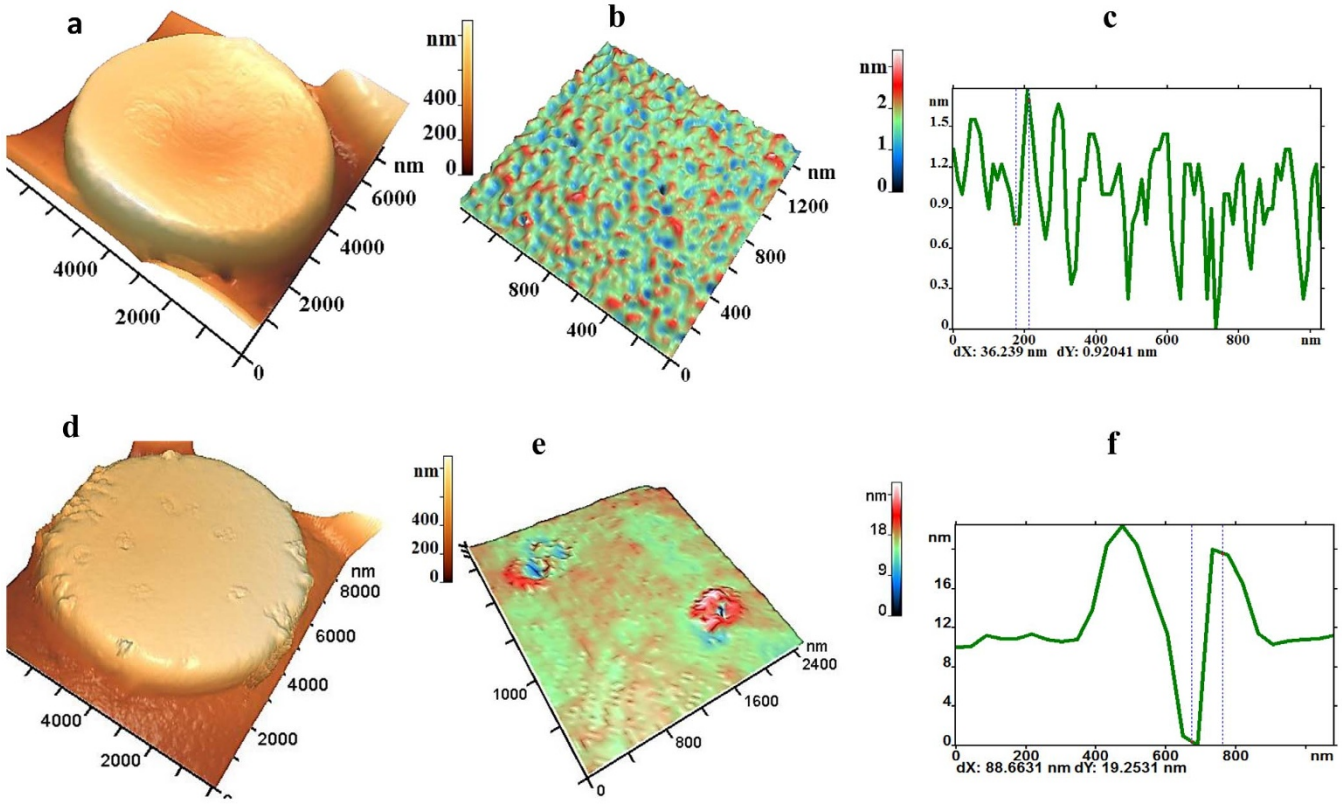

Figure 2 | The process of domains rising on the membrane under the hemin action. Comparison with the control. (a), (b),(c) For hemin concentration C=0 (control). (d), (e),(f) For hemin concentration C=1.1–1.2 mM. (a) and (d) The AFM 3D- images of RBCs 8 × 8 μm. (b) and (e) AFM 3D-images of membrane surfaces 1300 × 1300 nm (control) and 2400 × 2400 nm (surface with incipient domais). (c) and (f) Typical profiles of the surface in control membrane and in membrane with incipient domains. Interaction time of hemin with RBCs was 1 hour. The typical control cells were chosen out of the ensemble of 2820 cells, under the hemin action – out of 3010 cells. Membrane nanoscructure and profiles are represented as typical for given concentration and incubation time among 108 areas.

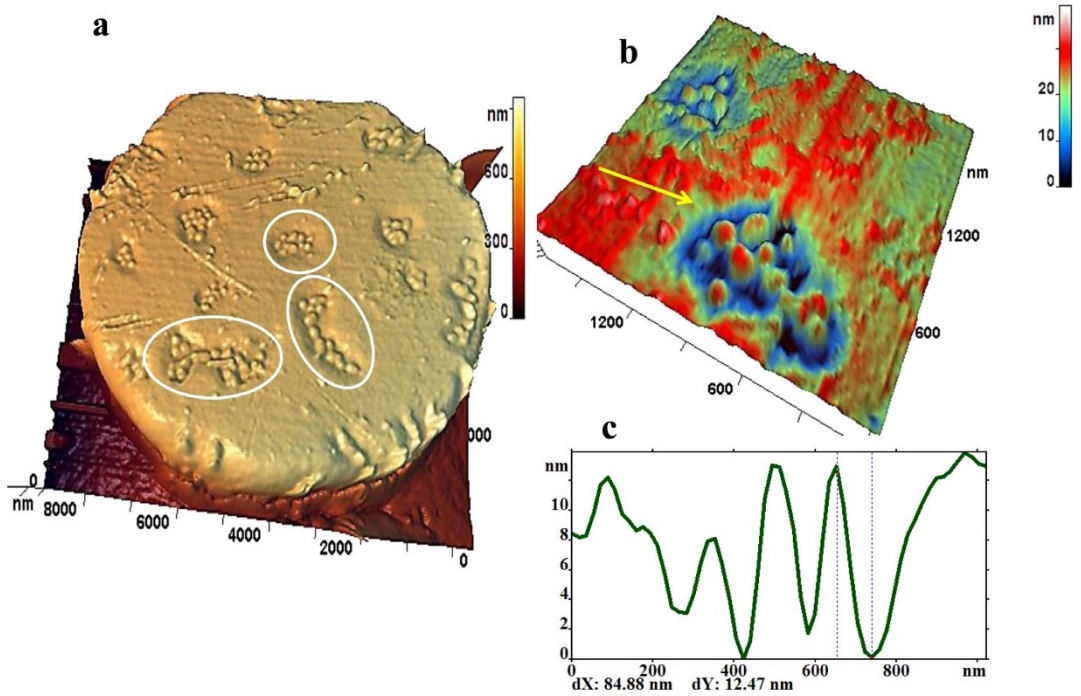

Figure 3 | Domains with "grain" structures on the membrane surface under the hemin action C = 1.5 mM. AFM images. (a) RBC 3D-image with "grains"-containing domains. White circles indicate the domains with "grains". (b) 3D- image 1500×1500 nm of "grains" in the domain, indicated by yellow arrow. (c) Profile of the domain structure. Interaction time of hemin with RBCs was 1 hour. Typical cells were chosen out of the ensemble of 3250 cells. Membrane nanoscructure and profiles are represented as the typical for given concentration and incubation time among 108 areas.

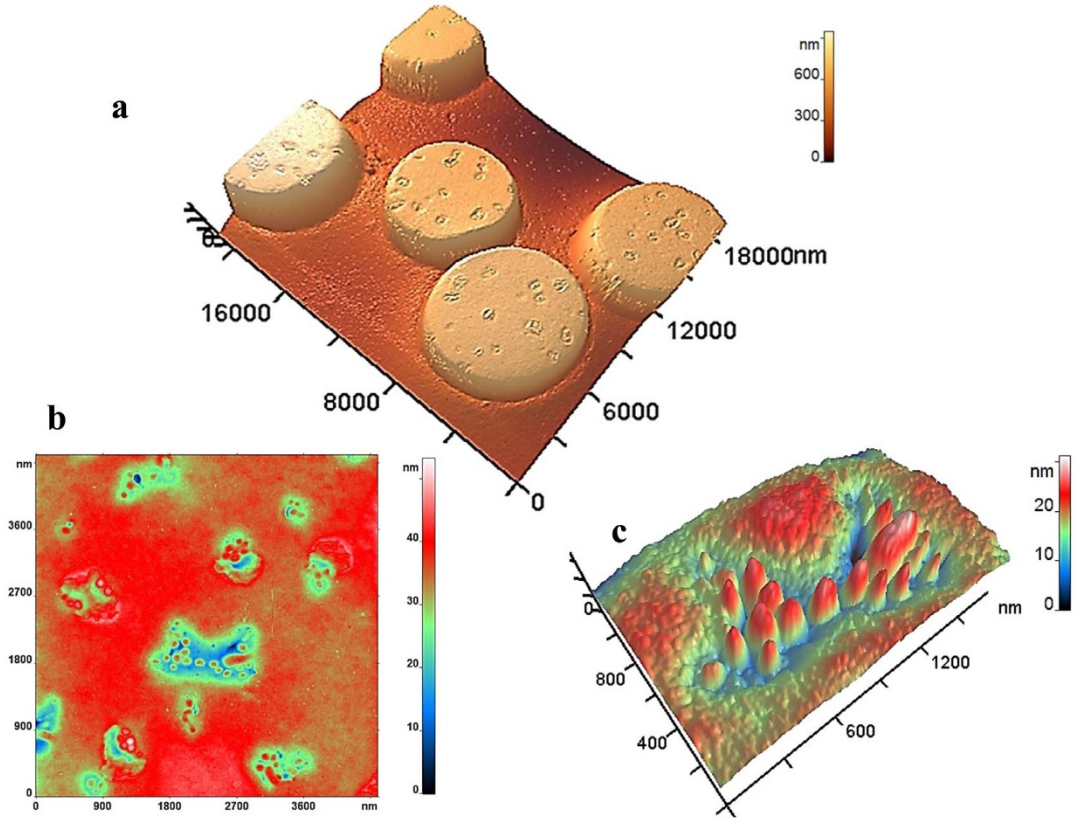

Figure 4 | Cells with "grain"-containing domains. (a) AFM 3D-image 18 × 18 μm of 5 cells with topologic defects in membrane in form of "grain"-containing domains. (b) Fragment of membrane with "grain"-containing domains, AFM 2D-image 4×4 μm. (c) "Grains" in a domain, AFM 3D-image 1500 × 1500 nm. Interaction time of hemin with RBCs was 1 hour, C = 1.5 mM. These cells were typical among 45 smears. Membrane nanoscructure is represented as typical for given concentration and incubation time among 108 areas of membrane surface.

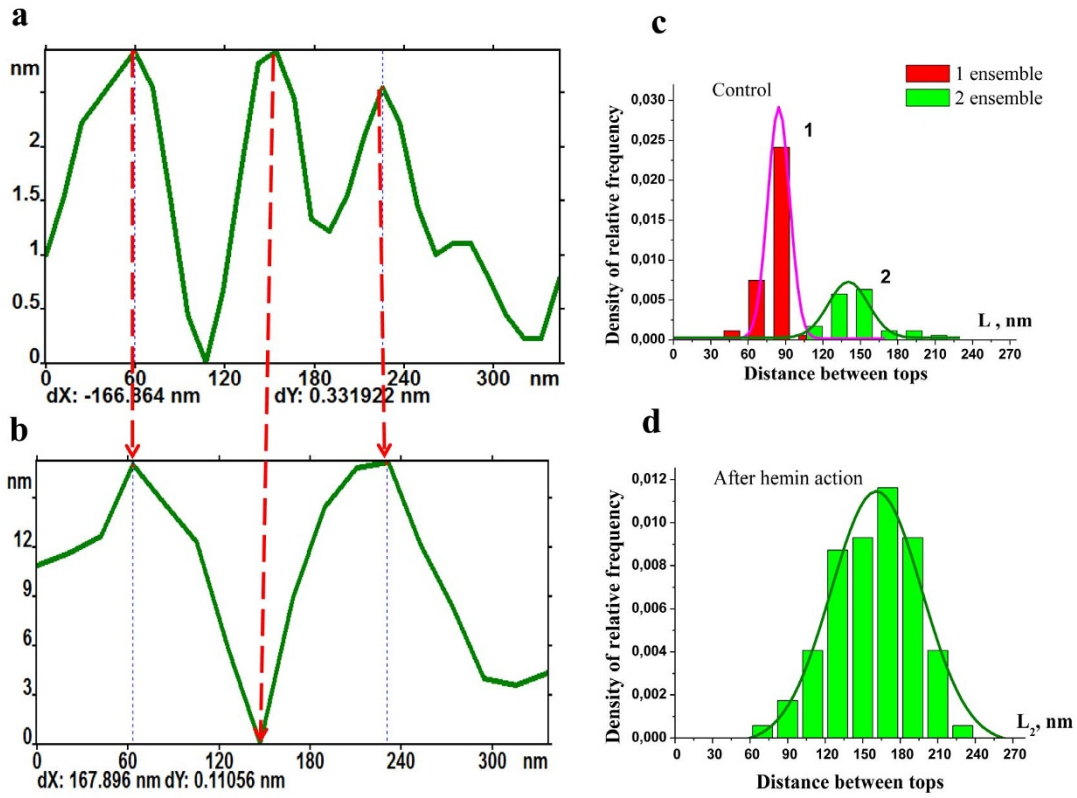

Figure 5 | Profiles and histograms of spatial periods of membrane nanostructures for the control cells and cells after the hemin action. (a) Profile of the control membrane. (b) Profile of the membrane surface in the domain. (s) Histogram of the spatial periods of structures for the control membrane. (d) Histogram of the spatial periods in the field of domains. Interaction time of hemin with RBCs was 1 hour, C = 1.5 mM. Profiles are represented as typical for given concentration and incubation time among 108 areas. Sample volume for control histograms was 310, after hemin action – 215.

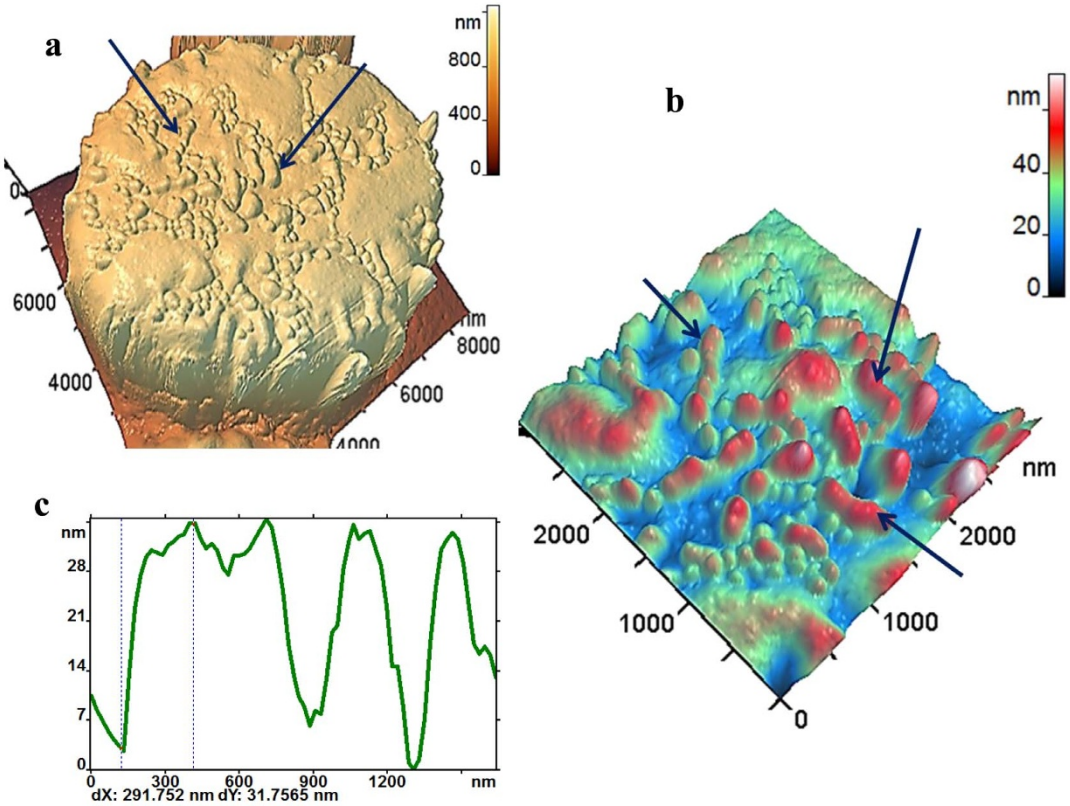

Figure 6 | Merging of "grains" in the domain. (a) RBC 3D- image – in its membrane partial merging of "grains" in a domain occurred (arrows). (b) 3D-image of the fragment of membrane surface with merged "grains" in domain (arrows). (c) Profile of this surface. Interaction time of hemin with RBCs was 1 hour, C=2.5 mM. Cells, membrane nanoscructure and profiles are represented as representative for given concentration and incubation time among 3120 cells.

when the hemin concentration was increased. The microscale characteristics of the fused topological patterns are L_f =900 ± 100 nm (Fig. 6). Separate and fused "grains" were simultaneously observed on the membrane surface (Fig. 6 a,b). The profile of the membrane surface in this case (Fig. 6c) was differed from that with "grains" (Fig. 3c).

The fusion of "grains" inside the domains as well as the fusion of domains led to a formation of echinocytes and spheroechinocytes (Fig. 1e).

Discussion

The current study determined the formation of domains containing "grains" under the hemin action in a whole blood. The heterogeneity of the observed patch-like domains could result from several causes. Firstly, RBC are unequal in shape and age which could be critical for the formation of intramembrane supramolecular components with different sensitivity to damage. Secondly, a membrane-associated hemin could be heterogeneously distributed in the membrane due to a lower or higher plasma components concentration close to the membrane surface and/or due to a different affinity of the hemin to heterogeneous supramolecular complexes in the membrane.

Surprisingly we observed ordered, periodical nanostructures on the RBC surface after their incubation with increasing concentrations of hemin. We did not use fixators to create RBC monolayers. This allowed us to preserve the native membrane structure.

The percentage of hemolyzed cells after incubation with hemin in our study was insignificant (1.4 ± 0.3% at C=1.5 mM and 2.3 ± 0.4% at C=2.5 mM for incubation time up to 3 hours). However, it was reported that 4% of RBC were hemolyzed 48 hrs after the incubation with hemin at C=10 μM[8]. In the latter experiments RBC were incubated in a Ringer solution. In our experiments, to protect RBC and maintain the natural microenvironment, the incubation with hemin was performed in a whole blood containing plasma proteins that protected blood cells from excessive damage in vitro.

Considering the mechanisms of formation and merging of the "grains" within the cell membrane surface a mathematical model was developed.

The of RBC consist of lipid bilayer and cytoskeleton network[16–17]. The spectrin network is coupled with the lipid bilayer through the transmembrane proteins. One linkage is made by ankyrin, which forms a bridge between the spectrin and the band 3[18–19]. A second skeleton-bilayer link is formed with the participation of protein 4.1R. The cell owes mechanical resilience due to membrane-associated protein skeleton. This has the form of a lattice, made up of spectrin tetramers. The tetramers are attached at their ends to predominantly six fold junctions[20].

In Fig. 7a the scanning image of the control membrane (no hemin, 800 × 800 nm) is shown. On this image the cantilever delineates the protein complexes, i.e. peaks and cavities on the cell membrane which correspond to the junctional complexes in a lipid membrane. The maximum contour length of the spectrin tetramer is estimated to be 200 nm[21]. However, the end-to-end distance of the tetramer was estimated to be 70 nm[21]. AFM images of RBCs under the physiological conditions showed the spectrin tetramer to be in a compressed state in the network, with an average length between 35 to 100 nm[22]. These findings indicated that in the resting state of RBC the average extension of the tetramer is only a fraction of its contour length[21]. Fig. 7 demonstrates an AFM image of a control cell surface (Fig. 7a), scheme of ankyrin complex (red-rose) and 4.1R complex (cyan-blue) (Fig. 7b) and the space profile (Fig. 7c) corresponding to the scheme and AFM image. The typical distance between maximum

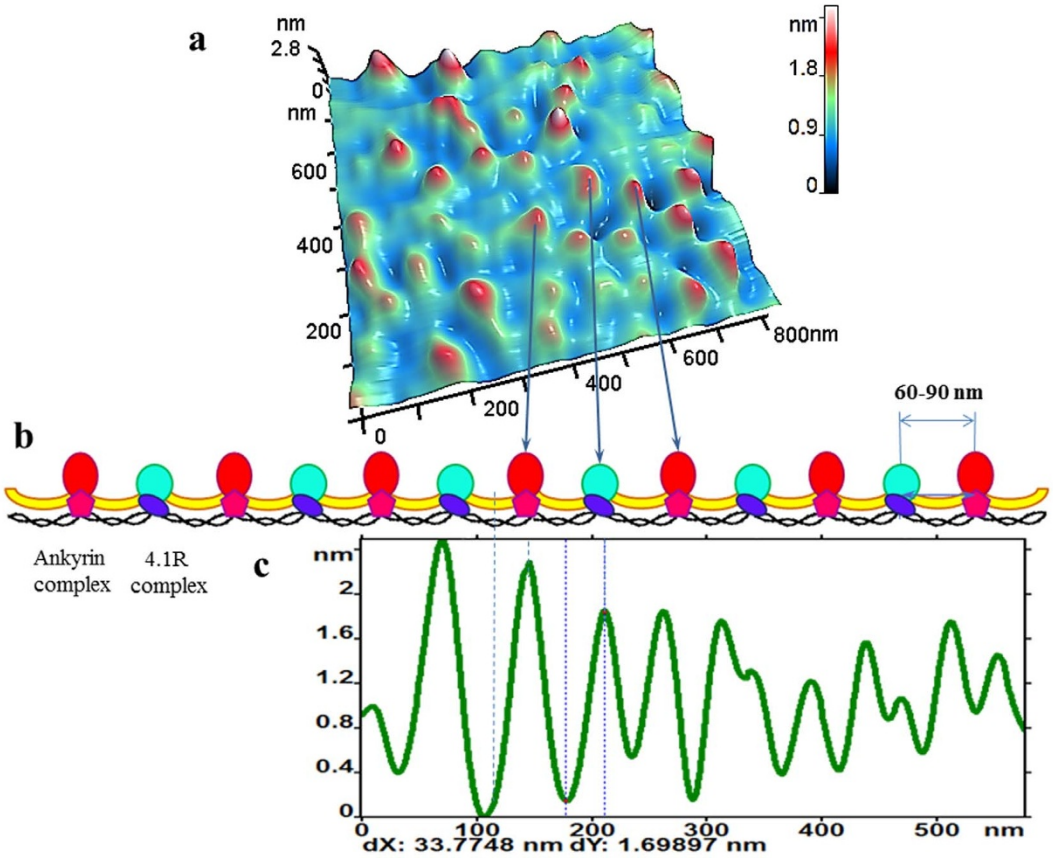

Figure 7 | Fragment of nanosurface of control cell, C=0. (a) AFM 3D- image of membrane nanosurface fragment 900 × 900 nm. (b) Model of profile. (c) AFM- profile in the adjusted section on the surface. Arrows show images of protein complexes in a model. Membrane nanoscructure and profiles are represented as typical for given concentration S=0 among 108 areas.

and minimum heights on the profile is 1.2 ± 0.8 nm, and the space period is L=80 ± 20 nm.

Under the hemin action the stage of "grain" formation on the membrane surface (Fig. 1d) was detected following the planocytes formation (Fig. 1c). Planocytes have larger diameter than discocytes. Probably their spectrin fibers were more stretched than in a discocyte.

The hemin can influence the membrane proteins. It is known that the influence of hemin on spectrin and protein 4.1 is significant while on actin - only minor[23]. Hemin could alter the conformation of protein 4.1 and weaken spectrin-protein 4.1 interaction and associations[4]. Protein 4.1R forms a complex with actin and spectrin, which defined the nodal junctions of the membrane-skeletal network. Defects or deficiency of components of the junctional complexes, and especially of 4.1R, led to an instability of the network[20]. The perturbation of this macromolecular complex contributed to remodeling the red cell surface[20].

Fig. 8 shows the model of interactions between the membrane proteins. Under the hemin action the interconnection between proteins 4.1 and spectrin, topologically correspondent to AFM image (Fig. 8a), weakened and disrupted (Fig. 8b and arrow 1).

The hemin is capable to alter the conformation of spectrin[24]. The hemin promotes dissociation of spectrin tetramers to dimers. Such an effect plays a role in the membrane flickering[17]. The dissociation of a spectrin filament is also the stage of creating topological defects in membrane[2]. This process is shown in Fig. 8b, arrow 2. Hemin inhibited the spectrin dimer-dimer association. A spectrin damage could also occur in an ankyrin complex[25]. No spectrin dissociation was detected with other porphyrin derivatives[4].

Due to the damages indicated by arrows 1 and 2 (Fig. 8b) the protein complexes 4.1 are locally descended (Fig. 8b), and ankyrin complexes are stayed on the surface. That is a mechanism of arising of topological grain-like defects on the membrane surface. We can assume that this process is a "vesiculation inside". In the AFM images red "grains" are shown (Fig. 8a), which correspond to red circles in the model (Fig. 8b). The tips and cavities in domain are shown on profile at a given cross-section of the membrane nanosurface (Fig. 8c). According to this mechanism the space period between the "grains" is about L=120–200 nm. These values were just observed in the experiment.

It should be noted that the formation of "grains" is the threshold concentration-dependent effect. The existence of a minimal hemin concentration causing the changes in RBC, in particular fast RBC hemolysis, was also described in the study[26]. At a high concentration of hemin "grains" in domains merged forming joint structures (Fig. 9a).

Structural models for the membrane skeleton suggest that the spectrin network is highly malleable and can exist in a stretched or compressed states. The hemin causes a transformation of tetramers into dimers. Spectrin dimers lost their rope-like structure and became shorter[4]. Vesiculation and formation of spheroechinocytes are also related to spectrin shortening[27]. The increase of spectrin oxidation during the storage of blood is associated with vesiculation[28].

In Fig. 9b the model of transformation of cavities into plane and convex structures ("vesiculation outside") is shown. This happed, probably, due to shortenings and cross-linking of spectrin filaments (arrow 3). This model corresponds the experimental data (Fig. 9 a,c). Fig. 9c shows the profile in the given cross-section, maximum and minimum on the profile are nearly merged.

The formation of "grains" is possible only at certain hemin concentrations and incubation time. Spectrin and protein 4.1 exhibited a

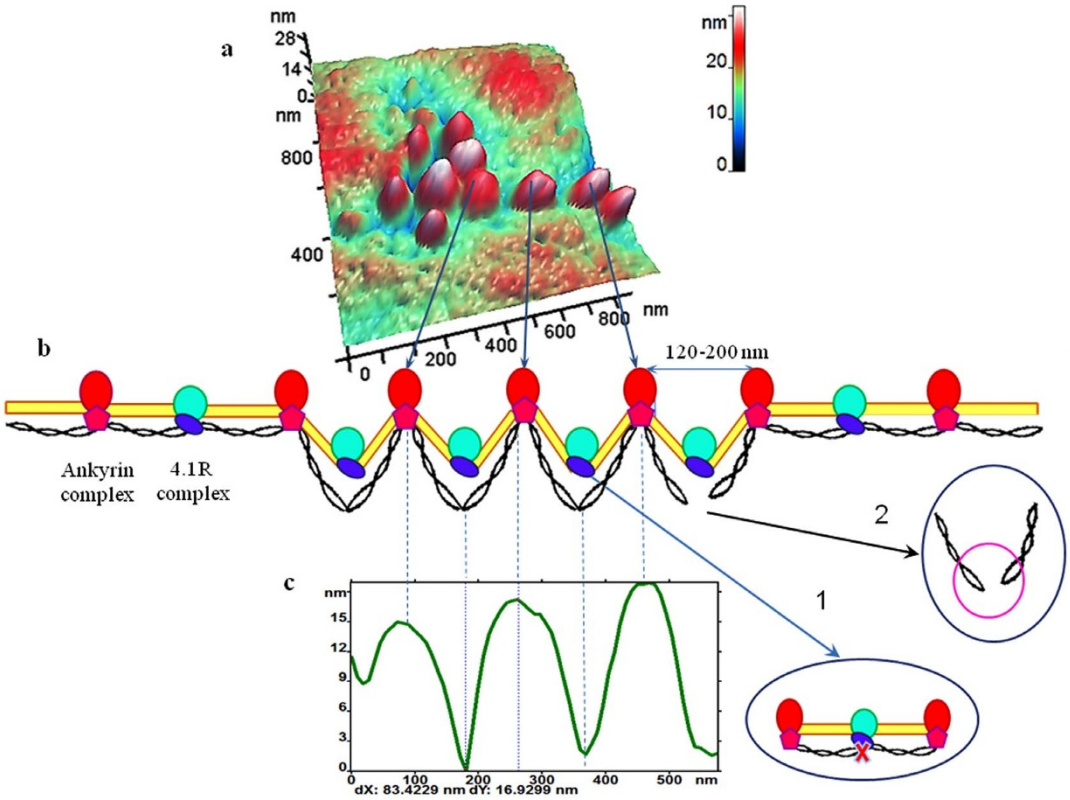

Figure 8 | Fragment of membrane surface of planocyte with "grain" structures after hemin action, C=1.5 mM. (a) AFM 3D- image of membrane nanosurface fragment 900 × 900 nm. (b) Model of profile. (c) AFM profile in the adjusted section on the surface. The region of rupture of connection *band 4.1R–spectrin* is shown by the arrow 1, rupture in spectrin is shown by arrow 2. Incubation time was 1 hour. Membrane nanostructure and profiles are represented as typical among 108 areas.

time-dependent increasing tendency to undergo hemin-induced peroxidative crosslinking. Cytoskeletons incubated with hemin lost their "cell like" shapes in a time dependent manner[3].

It is of interest to understand whether the hemin action is reversible. We suppose that it may be reversible as it was shown in our research in which we discovered that albumin could reverse the zinc ions effects on RBC membranes[14]. The study of membrane nanosurface may reveal mechanisms of hemolysis inhibition by vitamin *E* and other substances[29]. But this topic is out of the scope of this article.

In our experiments we detected various types of topologic defects on the membrane (Fig. 10b,c,d). They can be divided into 3 classes. Small – separate "grains" (Fig. 8a, Fig. 10b) have typical spatial period 120–200 nm. Medium – merged 2–5 "grains" (Fig. 9a and Fig. 10c), have spatial period 300–500 nm. Large – the result of merging of medium defects (Fig. 10d) have the size of 500–1500 nm. Let us discuss the kinetics of defects formation and transformation.

As noted above hemin may cause the disturbance of junction between the band 4.1 and spectrin, and also the rupture of spectrin filaments. These areas of membrane, where the disturbance of membrane surface can arise due to this mechanism, we call active centers (ac), as in the works[12,30]. Under the hemin action the weakest junctions damage initially. Topological defects in the form of "grains" defects arise. Then more junctions are distorted. The maximum amount of active centers is determined by the total number of all junctions N_{max} on the membrane.

Let us assume that the amount of active centers decreases with an incubation time according to exponential law:

$$N_{ac}(t) = N_{max} e^{-kt}, \tag{1}$$

where k is the rate constant which depends on the type of agent and its concentration.

Then the number of "grains" $n(t)$ will increase with time and will reach the maximum N_{max}:

$$n(t) = \alpha\left(1 - e^{-kt}\right), \tag{2}$$

here $\alpha = N_{max}$.

The rate of "grain" formation is

$$\frac{dn}{dt} = \alpha k e^{-kt}. \tag{3}$$

When spectrin shortens, the process of merging of several "grains" occurs (with the rate constant β) and the number of separated "grains" decreases. The process of formation and disappearance of "grains" will be described by the kinetic equation:

$$\frac{dn}{dt} = \alpha k e^{-kt} - \beta n. \tag{4}$$

Initial condition: for $t = 0$ $n = 0$, (5)

where: $\frac{dn}{dt}$ is the rate of change of "grain" number, $\alpha k e^{-kt}$ is the rate of formation of "grains", $-\beta n$ is the rate of decrease of "grains" due to merging of neighboring "grains".

Therefore the number of small defects depends on time:

$$n(t) = \frac{\alpha k}{\beta = k}\left(e^{-kt} - e^{-\beta t}\right). \tag{6}$$

This relation is shown in Fig. 10a (curve 1).

Medium defects form out of 2–3 small defects due to merging of "grains". The rate of their increase is proportional to the number of small defects $n(t)$. The rate of their decrease is proportional to the

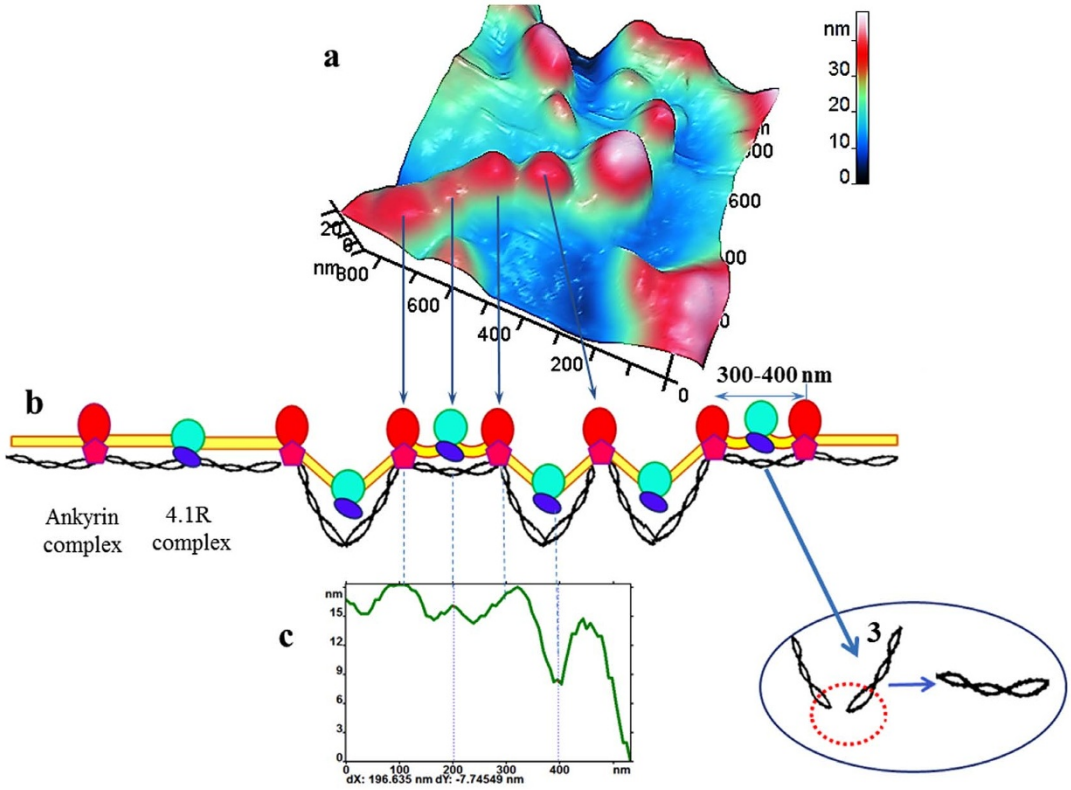

Figure 9 | Fragment of membrane surface with merged "grains" in the domain after hemin action, C=2.5 mM. (a) AFM 3D- image of the nanosurface fragment 900 × 900 nm. (b) Model of profile. (s) AFM profile in the adjusted section on the surface. Arrow 3 points on the process of crosslinking of spectrin filament. Incubation time was 1 hour. Membrane nanoscructure and profiles are represented as typical among 108 areas.

number of medium defects $N(t)$ (with the rate constant γ). These two processes are represented in equation by the first and second summands correspondingly:

$$\frac{dN}{dt} = \frac{\beta\alpha k}{\beta - k}\left(e^{-kt} - e^{-\beta t}\right) - \gamma N. \tag{7}$$

Solving the equation, we obtained:

$$N(t) = \frac{\beta\alpha k}{(\beta-k)(\gamma-k)}e^{-kt} - \frac{\beta\alpha k}{(\beta-k)(\gamma-\beta)}e^{-\beta t} + \left(\frac{\beta\alpha k}{(\beta-k)(\gamma-\beta)} - \frac{\beta\alpha k}{(\beta-k)(\gamma-k)}\right)e^{-\gamma t}. \tag{8}$$

This dependence $N(t)$ is shown in Fig. 10a (curve 2).

The images of small, medium and large defects are shown in Fig. 10 b,c,d. The amount of small defects at first increases with time (Fig. 10a, curve 1). The AFM image represented in Fig 10b, corresponds to this stage. Then due to the merging the number of small defects ("grains") decreases (Fig. 10a, curve 1), and the amount of medium defects increases (Fig. 10a, curve 2). Then they start to merge and their amount decreases. And as a result there is the moment when the function $n(t)$ have the maximum. For the curve, represented in Fig. 10a $t=1.3$ (relative units). At a time moment $t=3.2$ the amount of small and large defects are equaled. The AFM image at this time point is shown in Fig. 10c. In this AFM image the separated and merged "grains" are visible simultaneously. Their amount is just about the same on the image. The amount of medium defects $N(t)$ also has maximum, but it is delayed relatively to the $n(t)$ maximum (Fig. 10a,d). The graphic presentation of these relations is well-corresponded to the experimental data, discussed in this study.

Conclusion

The nanostructure of the membrane surface of RBC after the hemin exposure was investigated. The nanostructure of "grain" - containing domains was thoroughly discussed. The membrane structure was depended on the hemin concentration and incubation time. The role of spectrin matrix in the formation of domains in the current model was discussed.

Having analyzed the statistical ensembles of RBC we made a conclusion about the stages of changes of their shapes and membrane nanosurfaces. The processes of transformation of local topological nanoscale defects of RBC membrane into microscale defects, and finally into the RBC morphology change (echinocytes and spheroechinocytes) were studied. The analysis of the kinetics of local topological defects formation was based on experimental data of sizes of "grains" arising after hemin action on spectrin and protein complexes. The kinetic equations of formation and transformation of small $n(t)$ and medium $N(t)$ topological defects in membrane were suggested.

The AFM study of the dynamics of alterations of RBC membrane nanosurface and the mathematical model can be used in experimental biology and medicine for the analysis of the action of various agents on RBC membranes.

Methods

Blood and solutions. The blood withdrawal (200 μl) was performed from five donors into microvettes with EDTA (Sarstedt AG & Co., Nümbrecht, Germany). Hemin (Sigma-Aldrich, MO, USA) was used to make the base solution. 50 mg of hemin powder was dissolved in 1 ml 0.5 M NaOH in distilled water. To develop working solution, the base solution was further diluted (1 part of base solution plus 5 parts of distilled water). The working solution of hemin was added to the microvettes containing whole blood specimen to get the final concentrations within the range of 0.3–2.5 mM. The incubation time varied from 3 min to 180 min.

Preparations of all solutions, hemin incubation, smears preparations, AFM scanning in the current research were performed under the temperature of 19–20°C.

Ethics review. The study was performed in accordance with the principles of the Declaration of Helsinki and was approved by the Ethics Committee of V.A. Negovsky Scientific Research Institute of General Reanimatology, Moscow, Russian Federation. An informed consent was obtained from each participant prior to the study.

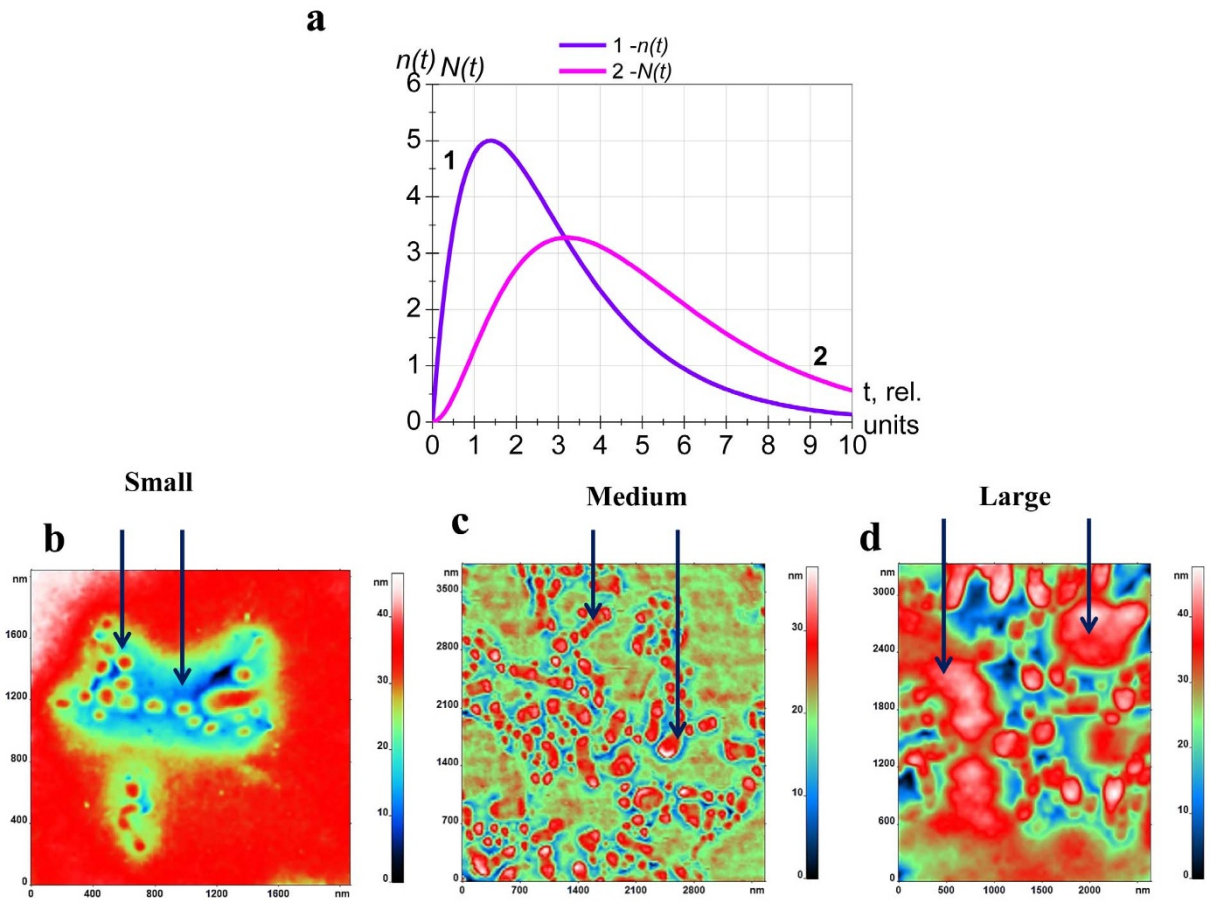

Figure 10 | **Kinetics of formation and development of topologic defects.** (a) Theoretical curves of dependences of the number of small defects (''grains'') on time *n(t)* and of the number of medium defects (merged ''grains'') on time *N (t)*. (b–d) - AFM 2D- image of membrane surface: small – separate ''grains'' in domains (b), medium – merged ''grains'' in domains (c), large – merging of domains. (d). Values *t*, *n(t)* and *N(t)* are in relative units.

Atomic force microscopy. The AFM method was used to study the dynamics of morphological alterations of RBC membrane patterns at the nanoscale level. Previous studies proved the informative value of AFM imaging for observing the details of the membrane nanostructure following various physical and chemical agents[1,13–15,31–32]. In our experiments cells were scanned by the AFM "NTEGRA Prima" (NT-MDT Co., Zelenograd, Moscow, Russian Federation) under the semi-contact mode. Cantilevers NSG01 (NT-MDT Co., Zelenograd, Moscow, Russian Federation) with force constant 5 N/m, tip curvature radius 10 nm, resonant frequency 190 kHz were used. The number of scanning points were 512 or 1024 within each line of image.

Monolayers of RBCs on glass slide were prepared with the aid of blood smear preparation device, the model V-Sampler (West Medica Produktions- und Handels GmbH, Vision, Austria) prior to AFM scanning. For each hemin concentration and incubation time three smears were prepared with a monolayer area of 1.5×1.5 cm each.

To analyze the shapes of cells in monolayers 3 areas 100 × 100 μm from each smear were randomly chosen and scanned. The experiments were repeated 5 times. Thus for each hemin concentration and incubation time 45 images including 60–100 cells each were analyzed. More detailed images were developed by scanning fields of 30 × 30 μm. For each hemin concentration and incubation time the percentage of cells of different types were estimated and statistically processed. For given parameters the representative (typical) cells forming more than 70% of monolayer were selected.

For the analysis of a membrane surface of representative cells the scanned fields of 30 × 30 μm were subdivided into the areas of 10 × 10 μm each containing one RBC and scanned again by AFM. Totally 12 cells per each of three smears were scanned. To get high resolution of the AFM images the optimal number of scanning points were estimated as 1024. Afterwards 3 areas of the cell membrane (1000 × 1000 nm) were selected in each cell and therefore 108 images were obtained by the AFM. The typical membrane parameters of each image were quantified by the software FemtoScan Online (Advanced Technologies Center, Moscow, Russian Federation).

There are own membrane parameters of nanosurface[1,13,33]. To characterize the membrane topology the spatial Fourier analysis was used to decompose the image of the membrane surface into three constituents based on space periods of membrane patterns revealed by AFM[1,34]. This methodological approach was proposed and described in detail in our previous studies[1,13].

Statistical analysis. The data were statistically processed by Origin 6.1. (OriginLab Corporation, MA).The one-way ANOVA was used, $p<0.05$ was considered statistically significant.

1. Moroz, V. V. *et al.* Comparison of red blood cell membrane microstructure after different physicochemical influences: atomic force microscope research. *J. Crit. Care* **25**, 539.e1–539.e12 (2010).
2. Gov, N. S. & Safran, S. A. Red blood cell membrane fluctuations and shape controlled by ATP-induced cytoskeletal defects. *Biophys. J.* **88**, 1859–1874 (2005).
3. Shaklai, N., Avissar, N., Rabizadeh, E. & Shaklai, M. Disintegration of red cell membrane cytoskeleton by hemin. *Biochem. Int.* **13**, 467–477 (1986).
4. Liu, S. C., Zhai, S., Lawler, J. & Palek, J. Hemin-mediated dissociation of erythrocyte membrane skeletal proteins. *J. Biol. Chem.* **260**, 12234–12239 (1985).
5. Wyse, J. W. & Butterfield, D. A. Interaction of hemin with erythrocyte membranes: alterations in the physical state of the major sialoglycoprotein. *Biochim. Biophys. Acta* **979**, 121–126 (1989).
6. Becker, P. S., Cohen, C. M. & Lux, S. E. The effect of mild diamide oxidation on the structure and function of human erythrocyte spectrin. *J. Biol. Chem.* **261**, 4620–4628 (1986).
7. Chiu, D. T. *et al.* Hemin-induced membrane sulfhydryl oxidation: possible involvement of thiyl radicals. *Free Radic. Res.* **27**, 55–62 (1997).
8. Gatidis, S., Föller, M. & Lang, F. Hemin-induced suicidal erythrocyte death. *Ann. Hematol.* **88**, 721–726 (2009).
9. Belcher, J. D., Beckman, J. D., Balla, G., Balla, J. & Vercellotti, G. Heme degradation and vascular injury. *Antioxid. Redox Signal.* **12**, 233–248 (2010).
10. Pizzolato, P. Formalin pigment (acid hematin) and related pigments. *Am. J. Med. Technol.* **42**, 436–440 (1976).
11. Solar, I., Muller-Eberhard, U., Shviro, Y. & Shaklai, N. Long-term intercalation of residual hemin in erythrocyte membranes distorts the cell. *Biochim. Biophys. Acta* **1062**, 51–58 (1991).
12. Kozlova, E. K. *et al.* The diagnostic of membranes' state after exposure of gamma-radiation of small doses. *Radiats. Biol. Radioecol.* **45**, 653–656 (2005).
13. Kozlova, E. K., Chernysh, A. M., Moroz, V. V. & Kuzovlev, A. N. Analysis of nanostructure of red blood cells membranes by space Fourier transform of AFM images. *Micron* **44**, 218–227 (2013).

14. Chernysh, A. M. *et al.* Reversible zinc-induced injuries to erythrocyte membrane nanostructure. *Bull. Exp. Biol. Med.* **154**, 84–88 (2012).
15. Kozlova, E. *et al.* Opposite effects of electroporation of red blood cell membranes under the influence of zinc ions. *Acta Bioeng. Biomech.* **14**, 3–13 (2012).
16. Kodippili, G. C. *et al.* Imaging of the diffusion of single band 3 molecules on normal and mutant erythrocytes. *Blood* **113**, 6237–6245 (2009).
17. Mohandas, N. & Gallagher, P. G. Red cell membrane: past, present, and future. *Blood* **112**, 3939–3948 (2008).
18. Thevenin, B. J., Willardson, B. M. & Low, P. S. The redox state of cysteines 201 and 317 of the erythrocyte anion exchanger is critical for ankyrin binding. *J. Biol. Chem.* **264**, 15886–15892 (1989).
19. Willardson, B. M. *et. al.* Localization of the ankyrin-binding site on erythrocyte membrane protein, band 3. *J. Biol. Chem.* **264**, 15893–15899 (1989).
20. Salomao, M. *et al.* Protein 4.1R-dependent multiprotein complex: new insights into the structural organization of the red blood cell membrane. *Proc. Natl. Acad. Sci. U.S.A.* **105**, 8026–8031 (2008).
21. Mirijanian, D. T. & Voth, G. A. Unique elastic properties of the spectrin tetramer as revealed by multiscale coarse-grained modeling. *Proc. Natl. Acad. Sci. U.S.A.* **105**, 1204–1208 (2008).
22. Swihart, A. H., Mikrut, J. M., Ketterson, J. B. & Macdonald, R. C. Atomic force microscopy of the erythrocyte membrane skeleton. *J. Microsc.* **204**, 212–225 (2001).
23. Solar, I., Dulitzky, J. & Shaklai, N. Hemin-promoted peroxidation of red cell cytoskeletal proteins. *Arch. Biochem. Biophys.* **283**, 81–89 (1990).
24. Lenormand, G., Hénon, S., Richert, A., Siméon, J. & Gallet, F. Elasticity of the human red blood cell skeleton. *Biorheology* **40**, 247–251 (2003).
25. Blanc, L. *et al.* Control of erythrocyte membrane-skeletal cohesion by the spectrin-membrane linkage. *Biochemistry* **49**, 4516–4523 (2010).
26. Iamaĭkina, I. V. & Chernitskiĭ, E. A. Hemolysis of human erythrocytes by hemin. The role of hemin in erythrocyte autohemolysis. *Biofizika* **39**, 691–694 (1994).
27. Eber, S. & Lux, S. E. Hereditary spherocytosis -- defects in proteins that connect the membrane skeleton to the lipid bilayer. *Semin. Hematol.* **41**, 118–141 (2004).
28. Wagner, G. M., Chiu, D. T., Qju, J. H., Heath, R. H. & Lubin, B. H. Spectrin oxidation correlates with membrane vesiculation in stored RBCs. *Blood* **69**, 1777–1781 (1987).
29. Wang, F., Wang, T., Lai, J., Li, M. & Zou, C. Vitamin E inhibits hemolysis induced by hemin as a membrane stabilizer. *Biochem. Pharmacol.* **71**, 799–805 (2006).
30. Kozlov, A. P. *et al.* Investigation of erythrocyte membrane damage under the action of γ radiation in a wide dose range using electroporation. *Physics of Particles and Nuclei Letters* **5**, 127–130 (2008).
31. Chernysh, A. M. *et al.* Erythrocyte membrane surface after calibrated electroporation: visualization by atomic force microscopy. *Bull. Exp. Biol. Med.* **148**, 455–460 (2009).
32. Moroz, V. V. *et al.* Macro- and microstructure of erythrocyte membranes under acute massive hemorrhage and subsequent blood reinfusion. *Semin. Cardiothorac. Vasc. Anesth.* **14**, 248–255 (2010).
33. Girasole, M. *et al.* Roughness of the plasma membrane as an independent morphological parameter to study RBCs: a quantitative atomic force microscopy investigation. *Biochim. Biophys. Acta* **1768**, 1268–1276 (2007).
34. Pretorius, E., du Plooy, J. N., Soma, P., Keyser, I. & Buys, A. V. Smoking and fluidity of erythrocyte membranes: a high resolution scanning electron and atomic force microscopy investigation. *Nitric Oxide* **35**, 42–46 (2013).

Acknowledgments

We thank colleagues of Scientific Research Institute of General Reanimatology RAS Bushueva Alexandra and Malahova Svetlana for their assistance in the experiments.

Author contributions

A.C. and E.K. suggested the idea to use hemin as the modifier of membrane nanosurface, designed the experiments. O.G., V.S. and E.K. conducted the experiments. O.G. and V.S. performed scanning by AFM, processed images by AFM soft, prepared figures. V.M., A.C. and A.K. discussed results and interpreted data. E.K. and A.C. suggested mechanism and mathematical model. E.K. and A.C. wrote the main manuscript text together with A.K. All authors reviewed the manuscript.

Additional information

Competing financial interests: The authors declare no competing financial interests.

How to cite this article: Kozlova, E. *et al.* Transformation of membrane nanosurface of red blood cells under hemin action. *Sci. Rep.* **4**, 6033; DOI:10.1038/srep06033 (2014).

This work is licensed under a Creative Commons Attribution-NonCommercial-NoDerivs 4.0 International License. The images or other third party material in this article are included in the article's Creative Commons license, unless indicated otherwise in the credit line; if the material is not included under the Creative Commons license, users will need to obtain permission from the license holder in order to reproduce the material. To view a copy of this license, visit http://creativecommons.org/licenses/by-nc-nd/4.0/